

Research Article

The surface nanostructures of titanium alloy regulate the proliferation of endothelial cells

Min Lai¹, Xiaofang Yang², Qing Liu², Jinghua Li¹, Yanhua Hou¹, Xiuyong Chen¹ and Kaiyong Cai^{1*}

¹ Key Laboratory of Biorheological Science and Technology, Ministry of Education, College of Bioengineering, Chongqing University, Chongqing 400044, China

² School of Materials Science and Engineering, Chongqing University, Chongqing 400044, China

* **Correspondence:** Email: kaiyong_cai@cqu.edu.cn; Tel: +86-23-65102507;
Fax: +86-23-65102877

Abstract: To investigate the effect of surface nanostructures on the behaviors of human umbilical vein endothelial cells (HUVECs), surface nanostructured titanium alloy (Ti-3Zr2Sn-3Mo-25Nb, TLM) was fabricated by surface mechanical attrition treatment (SMAT) technique. Field emission scanning electron microscopy (FE-SEM), atomic force microscopy (AFM), transmission electron microscopy (TEM) and X-ray diffraction (XRD) were employed to characterize the surface nanostructures of the TLM, respectively. The results demonstrated that nano-crystalline structures with several tens of nanometers were formed on the surface of TLM substrates. The HUVECs grown onto the surface nanostructured TLM spread well and expressed more vinculin around the edges of cells. More importantly, HUVECs grown onto the surface nanostructured TLM displayed significantly higher ($p < 0.01$ or $p < 0.05$) cell adhesion and viabilities than those of native titanium alloy. HUVECs cultured on the surface nanostructured titanium alloy displayed significantly higher ($p < 0.01$ or $p < 0.05$) productions of nitric oxide (NO) and prostacyclin (PGI₂) than those of native titanium alloy, respectively. This study provides an alternative for the development of titanium alloy based vascular stents.

Keywords: titanium alloy; human umbilical vein endothelial cells; SMAT; nanostructure; cell behavior.

1. Introduction

Due to the increasing prevalence of vascular diseases (such as coronary artery disease), it is urgent to develop vascular grafts with high efficiency [1]. In a clinical application, the failure of cardiovascular grafts was mainly contributed to thrombosis, which was induced by the activation or dysfunction of endothelial cells (ECs). Thus, how to regulate the ECs behaviors is essentially important for the development of vascular devices.

Cell behaviors at cell-material interfaces are highly regulated by surface property of a material, such as surface energy, surface chemistry, wettability, roughness and topography [2-5]. In particular, nanoscale structure of a material was confirmed to be an important factor to regulate cell behaviors, including cell adhesion, proliferation and differentiation [6]. Recently, more and more attention was attracted in respect to nanoscale surface engineering to mimic the natural nano-surface architecture of vascular tissue for the regulation of cellular responses. It has been demonstrated that the random nano-structures could promote the proliferation of endothelial cells [7] and vascular smooth muscle cells [8], respectively. Choudhary et al. [9] confirmed that nanostructured titanium produced by powder metallurgy technique greatly improved the behaviors of vascular cells. Liliensiek et al. [10] found that the behaviors of human vascular endothelial cells were regulated by nanotopography. However, it still needs further investigation to understand the interactions between endothelial cells and nanostructured surfaces.

Titanium alloys were commonly used as cardiovascular implants (ventricular device, total artificial hearts and circulatory devices, etc.) because of their superior physiochemical properties. Previously, TLM (Ti-3Zr2Sn-3Mo-25Nb) alloy, a nearly β -type titanium alloy, was successfully used as a vascular stent due to its high fatigue strength, lower elastic modulus and high plastic toughness [11-13]. Even though, TLM alloy has only limited biocompatibility due to its inherent bioinert property.

To this end, we fabricated surface nanostructure of TLM by surface mechanical attrition treatment (SMAT), in an effort to improve its interaction with cells. SMAT technique generally employs flying balls with high velocity to impact against the surface of a bulk material, leading to severe plastic deformation (SPD) with surface self-nanocrystallization [14,15]. After SMAT treatment, the surface nanostructured material exhibited good mechanical and wear resistant properties [16-18]. However, few studies [19-21] documented the cytocompatibility of SMAT treated TLM for biomedical applications.

The objective of this study was to fabricate surface nanostructured titanium alloy, and to investigate the influence of the surface nanostructured cue on the biological behaviors endothelial cells, including adhesion, proliferation, and function.

2. Materials and Method

2.1. Materials

The TLM (Ti-3Zr2Sn-3Mo-25Nb) alloy sheets were purchased from the Northwest Institute for Non-ferrous Metal Research (China). Hoechst 33258 and 3-(4, 5-Dimethylthiazol-2-yl)-2, 5-diphenyltetrazolium bromide (MTT) was purchased from Sigma Chemical (MO, USA). NO assay kit (catalogue no.: S0021) was purchased from Beyotime Biotechnology Co. (Jiangsu, China). PGI2

EIA kit was purchased from Enzo Life Sciences. (Postfach, Germany). Goat monoclonal antibody was provided by Santa Cruz Biotechnology (CA, USA). Fluorescein isothiocyanate (FITC)-conjugated mouse antigoat secondary antibody was purchased from ZSGB-BIO (Beijing, China). The rhodamine-phalloidin was provided by Invitrogen Co. (CA, USA).

2.2. Sample fabrication

Native TLM substrates were initially polished with diamond pastes (No. 800-2000). The polished TLM substrates were then washed with acetone, ethanol and double-distilled water each for 20 min and dried at 60 °C for 24 h. Both sides of titanium alloy sheets were treated with SMAT technique with steel balls (8 mm in diameter) with vibration frequency of 50 Hz. Each surface of a titanium alloy substrate was treated at room temperature for 60 min.

2.3. Sample characterizations

Metallurgical microscopy (PME, Olympus, Japan), field-emission scanning electron microscopy (SEM, FEINova 400 Nano SEM, Phillips, Holland) and atomic force microscopy (AFM, JPK Instruments AG, Germany-NanoWizard II) were employed to characterize the morphologies and structures of titanium alloy substrates, respectively. The X-ray diffraction (D/Max 2500PC, Rigaku, Japan) and transmission electron scanning (TEM, SUPRA, Zeiss, Germany) were used to reveal the crystalline structures of TLM substrates.

2.4. Cell culture

The Human umbilical vein endothelial cells (HUVECs) stored by freezing were re-suspended and seeded into the culture flask with RPMI1640 medium supplemented with 10% fetal bovine serum (FBS, Gibco) at 37 °C under 5% CO₂ atmosphere. At confluence, HUVECs were used for experiments.

2.5. Immunofluorescence staining

The staining was performed according to a previous study [21]. HUVECs were cultured onto all titanium alloy substrates (native or surface nanostructured ones) at an initial seeding density of 1×10^4 cells/cm². After culture for 12 h, HUVECs were fixed with glutaraldehyde (2 wt %) at 4 °C for 20 min. Next, samples were rinsed with PBS for 3 times and further treated with Triton X-100 (0.2 wt %) at 4 °C for 2 min. Then, the samples were rinsed with PBS for 3 times and incubated with mixture solution of bovine serum albumin (BSA, 1 wt %)/PBS at 37 °C for another 1 h. After that, goat monoclonal antibody against vinculin (1:200) was added and incubated at 4 °C for 24 h. Then, the fluorescein isothiocyanate (FITC)-conjugated mouse antigoat secondary antibody (1:100) was added and incubated at 37 °C for another 1 h. The samples were washed with PBS for 3 times and stained with rhodamine - phalloidin (5 U/mL) at 4 °C and incubated for 24 h. After that, the samples were counterstained with Hoechst 33258 (10 µg/mL) at ambient temperature for 5 min. Finally, the stained samples were mounted with glycerinum (90 wt %) and visualized with confocal laser scanning microscopy (CLSM, TCS SP5, Leica, Germany).

2.6. Cell adhesion and cell viability

To investigate the cell adhesion, HUVECs were seeded to native titanium alloy, and surface nanostructured titanium alloy substrates at an initial density of 2×10^4 cells/cm² and incubated at 37 °C for 1, 2 and 4 hours, respectively. The viability HUVECs cultured onto different substrates was evaluated with MTT assay. HUVECs were cultured on tissue culture polystyrene (TCPS) and different Ti substrates at an initial seeding density of 1×10^4 cells/cm² in a 24-well plate and incubated at 37 °C for 1 and 3 days, respectively. Then, 100 μ L of MTT substance (5 mg/mL) was added into each well and cultured at 37 °C for another 4 h. After that, cell culture medium was removed and adding 0.5 mL dimethyl sulfoxide (DMSO) into each well to dissolve formosan crystals. The solution's absorbance was then measured via a spectrophotometric microplate reader (Bio-Rad 680, USA) at a wavelength of 490 nm. Each sample was performed for five times.

2.7. Nitric oxide (NO) assay

NO assay was conducted using the Nitric Oxide Assay Kit according to the manufacturer's instructions. HUVECs were cultured on native titanium alloy, surface nanostructured titanium alloy and tissue culture polystyrene (TCPS) at a density of 1×10^4 cells/cm² for 1 and 3 days, respectively. Then, the supernatant was harvested and centrifuged at 1,500 g for 15 min to remove cellular debris. NO production in cells was measured by Griess method. The absorbance at 540 nm was measured using a spectrophotometric microplate reader (Bio-Rad 680). The NO concentration (expressed as μ mol mL⁻¹) was determined from a standard absorbance curve vs. a known concentration of NO run in parallel experiments.

2.8. PGI₂ assay

PGI₂ assay was performed with an EIA kit. HUVECs were cultured on native titanium alloy, surface nanostructured titanium alloy, and tissue culture polystyrene (TCPS) at a density of 1×10^4 cells/cm² for 1 and 3 days, respectively. Then, the supernatant was harvested and centrifuged at 1,500 g for 15 min to remove cellular debris. The amount of PGI₂ secreted in the supernatant was measured according to the manufacturer's instructions. The absorbance at 570 nm was measured using a spectrophotometric microplate reader (Bio-Rad 680). The PGI₂ concentration (expressed as μ g mL⁻¹) was determined from a standard absorbance curve vs. a known concentration of PGI₂ run in parallel experiments.

2.9. Statistical analysis

All data were presented as means with standard deviation (SD). The statistical analysis was analyzed by using software of OriginPro (version 6.1) via one-way analysis of variance (ANOVA) and Students's t-test. The confidence levels were set as 95% and 99%.

3. Results and discussion

3.1. Surface characterization

In this study, SMAT technique was employed to fabricate surface nanostructured titanium alloy

(TLM). The morphologies and crystalline structures of the native and surface nanostructured titanium alloy substrates were characterized with combined techniques of SEM, AFM, XRD and TEM, respectively.

From metallurgical microscopy observation, native TLM substrate displays relatively smooth surface morphology, however, with obvious scratches, which was derived from the polishing treatment. In contrast, surface nanostructured TLM substrate displayed rough surface morphology with coarse features (Figure 1 a vs b). Further SEM observation revealed that SMAT treatment led to the formation of nanograins ($\sim 20\text{--}70\text{ nm}$) on the surface of the treated TLM substrate (Figure 1 d vs c).

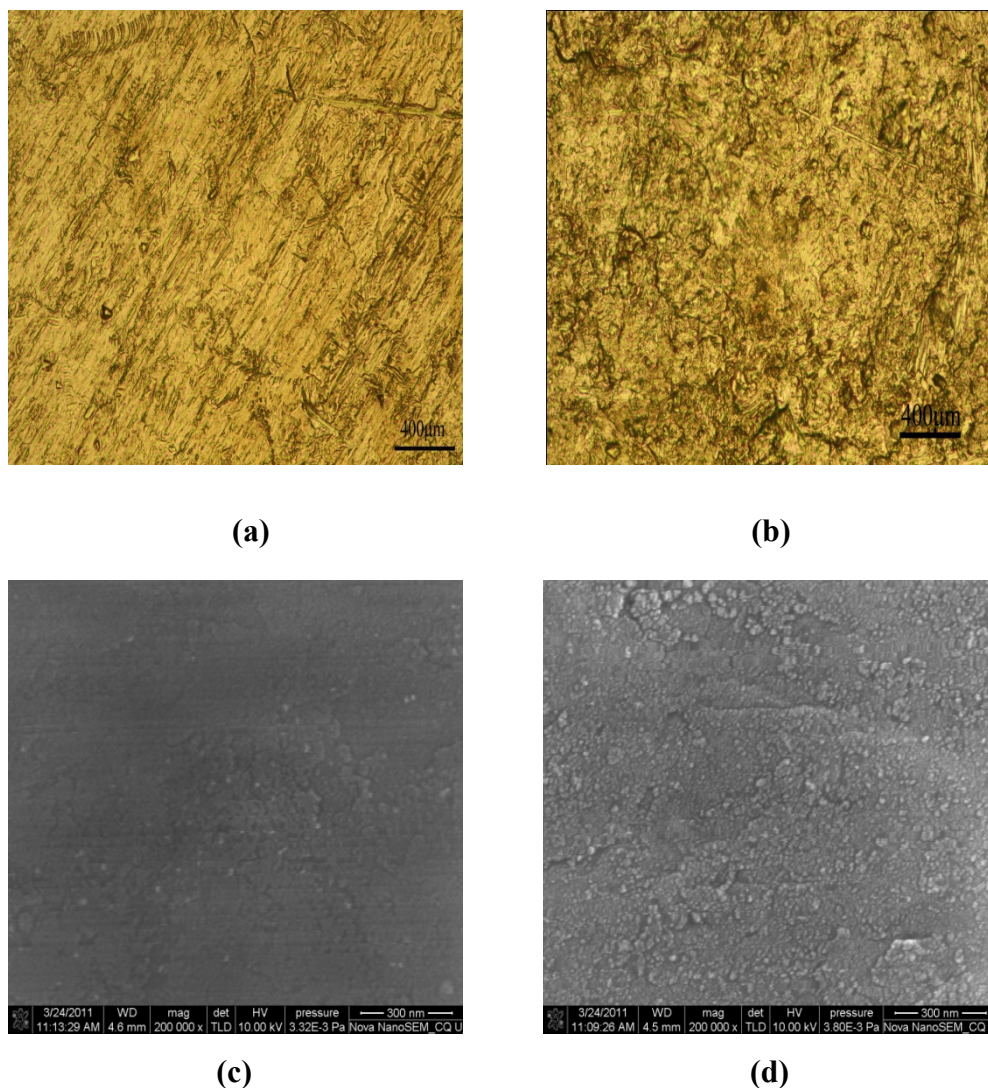


Figure 1. Representative optical micrographs of (a) native TLM substrate; (b) surface nanostructured TLM substrate, and SEM images of (c) native TLM substrate; (d) surface nanostructured TLM substrate.

To characterize the quantitative roughness of the TLM substrates, AFM measurements were then performed (Figure 2). The root mean square (RMS) roughness of the TLM substrates was

measured over an area of $1.5 \times 1.5 \mu\text{m}$. The RMS roughness value for native TLM substrate was round $6.487 \pm 1.47 \text{ nm}$ ($n = 4$) (Figure 2, a). After nanostructuring treatment with SMAT technique, the average RMS roughness of surface nanostructured TLM substrate increased to $19.66 \pm 5.45 \text{ nm}$ ($n = 4$). From the three-dimensional AFM observation, nanograins could be clearly observed (Figure 2, b). The result was consistent with that of SEM images.

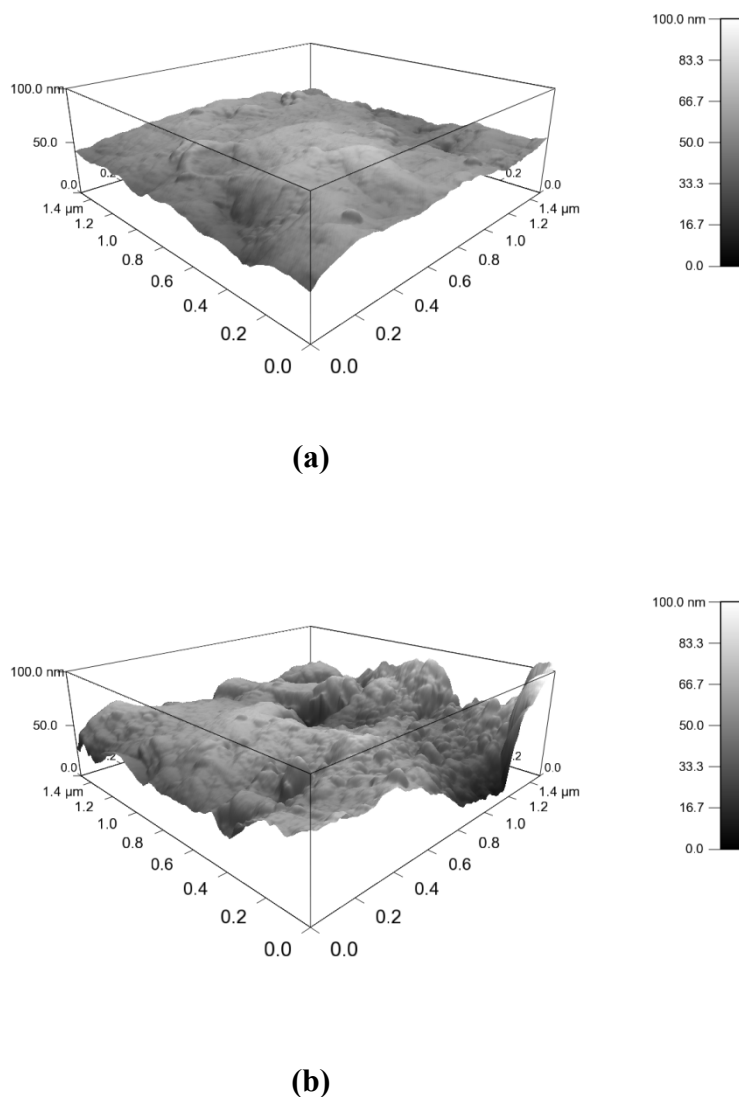


Figure 2. Representative AFM images of (a) native TLM substrate; and (b) surface nanostructured TLM substrate.

Next, we used TEM bright-field images and their corresponding selected area electron diffraction (SAED) patterns to characterize the nanocrystalline structures of the surface nanostructured titanium alloy substrates. We found that that nanograins with dimensions of around 20–70 nm with consistent crystallographic orientations were formed at a depth of 20–30 μm from the surfaces of SMAT treated TLM substrates (Figure 3).

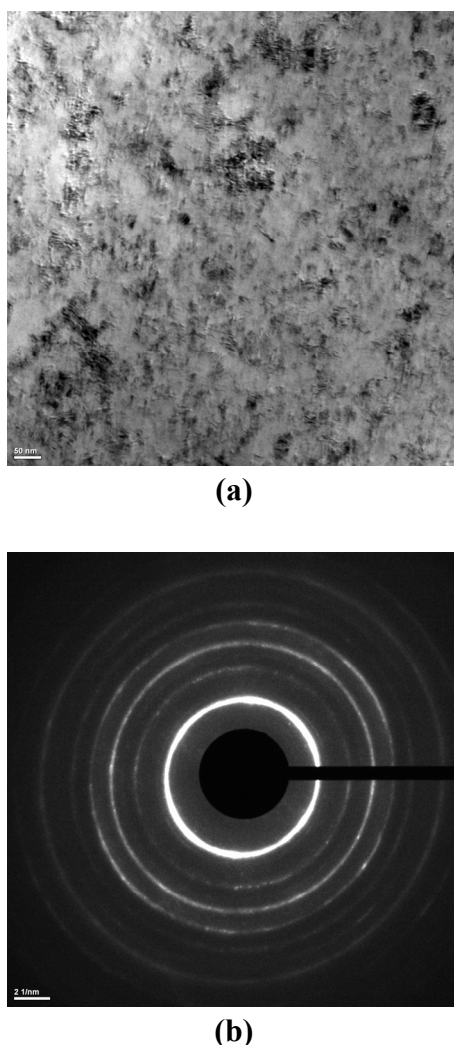


Figure 3. Representative TEM images of (a) bright-field view of the plane of surface nanostructured TLM substrate (surface); and (b) corresponding SAED pattern from sample (a).

To reveal crystal phases of native and SMAT treated TLM substrates, the x-ray diffraction (XRD) patterns of those substrates were recorded (Figure 4). Native TLM substrates demonstrated characteristic patterns of (110), (200), and (211) of β -Ti, with corresponding reflection peaks around $2\theta = 39^\circ$, 56° and 70° . The reflection peaks appearing around $2\theta = 35^\circ$, 53° and 63° , were assigned to patterns of (110), (102), and (110) of α -Ti (Figure 4, b). The results were consistent with previous reports [16, 21-23]. After treatment with SMAT technique, an additional signal was observed around 44° , which was assigned to the (101) pattern of α -Ti. The phenomenon could be interpreted that the surface activity of titanium substrates was improved after SMAT treatment; leading to the formation of TiO oxide in the presence of surrounding oxygen. The result was consistent with a previous study [24].

The result was consistent with previous studies [13,15,21]. Moreover, the diffraction peaks of the surface nanostructured TLM substrates became apparently broadened (Figure 4). It is related to the fact that the titanium substrate with grain refinement did not yield sufficient XRD signals to clearly identify the peaks, since the self- nanocrystallization process was occurred only at 20–30 μm

in depth from the surfaces of the TLM substrates.

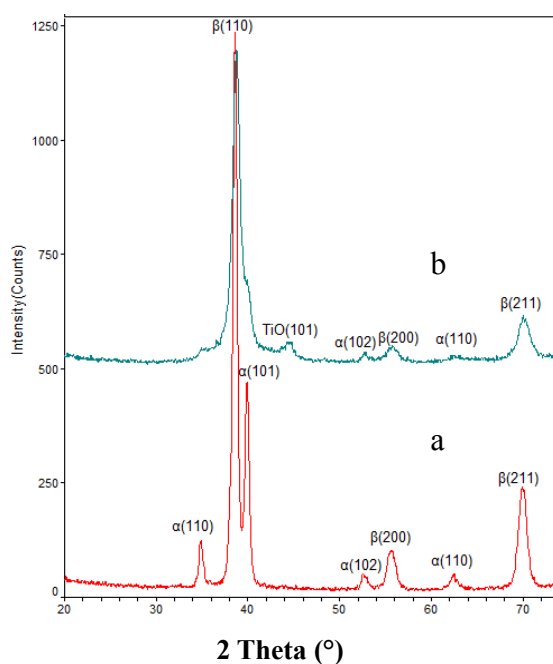
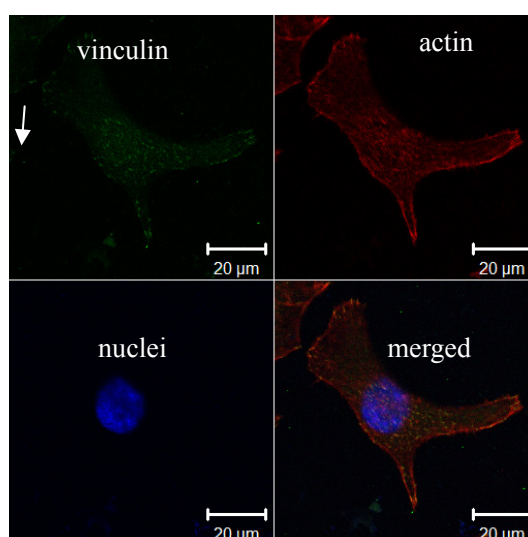


Figure 4. X-ray diffraction patterns of (a) native TLM substrate; and (b) surface nanostructured TLM substrate.

3.2. Cell morphology

Cell adhesion initially occurs when cells contact with the surface of a biomaterial. It then regulates subsequent cell behaviors, including cell proliferation, migration and differentiation etc. Vinculin, a focal adhesion protein, localized at specialized sites where microfilament bundles terminate at cell membranes, may participate in anchoring of microfilament bundles to specific membrane sites in various cells [25]. It directly reflects the cell adhesion.



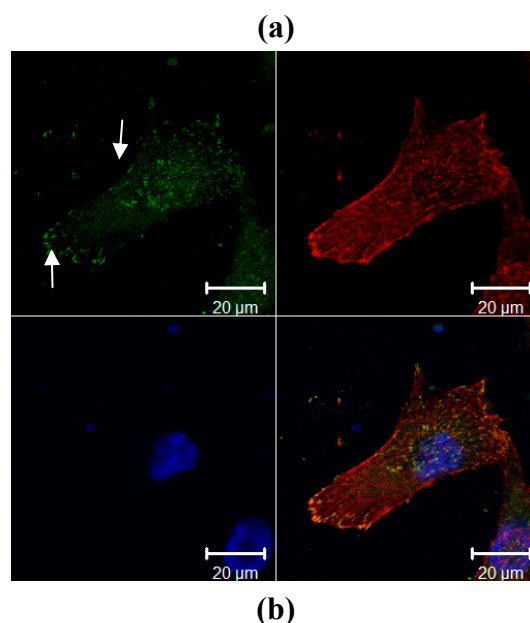


Figure 5. Fluorescent images of HUVEC adhered to (a) native TLM substrate; and (b) surface nanostructured TLM substrate; Cells were stained with actin filaments (red), cell nuclei (blue) and vinculin (green) in this study. Scale bar = 20 μ m.

To investigate the adhesion of HUVECs grown on native and surface nanostructured titanium alloys after 12 hours of culture, the actin, vinculin, and nuclei of HUVECs were visualized by immunocytochemistry. The HUVECs cultured onto surface nanostructured TLM substrates showed oval-shape morphology and more vinculin in a form of spots (arrows) were expressed around the boundaries of HUVECs comparing with that of native TLM substrates (Figure 5 b vs a). The result suggests that the surface nanostructuring treatment via SMAT enhanced the cell adhesion. It was consistent with a previous study [26]. The potential mechanism lies in that the SMAT treatment increases the fraction of grain boundaries of TLM substrates, and affects the conformation of the absorbed proteins, and in turn regulates cell behaviors. For instance, Webster et al. [27] demonstrated that surface nanostructures could affect the conformation of the absorbed proteins that allowed for the pro-adhesive motifs, such as RGD, to be accessible by the integrins of HUVECs. The enhanced adhesion of the HUVECs may positively influence the cell proliferation and biological functions.

3.3. Cell attachment and viability

To characterize the cell attachments and viabilities of HUVECs grown onto the native TLM, surface nanostructured TLM substrates, and tissue culture polystyrene (TCPS), MTT assay was performed in the present study. In an MTT assay, only viable cells could convert the yellow MTT substance into dark blue formazan crystals. Thus, we could evaluate the production of formazan and indirectly imply the initial attachments and viabilities of cells. The attachments of HUVECs on surface nanostructure titanium alloy substrate were significantly higher ($p < 0.05$) than those on native titanium alloy at the initial 4 hours of culture (Figure 6 a). Figure 6 b displays the viabilities of HUVECs adhered to different TLM substrates. After culture for 1 and 3 days, HUVECs cultured onto the surface nanostructured TLM substrates displayed significantly higher ($p < 0.05$ or $p < 0.01$)

viabilities than those of native TLM substrates, respectively. The result indicates that the proliferation of HUVECs was positively influenced by the nanograins structures of the substrates. Cell proliferation is the basis for subsequent cellular function, the improved proliferation of HUVECs along with a higher level of vinculin expression might significantly enhance cell functions.

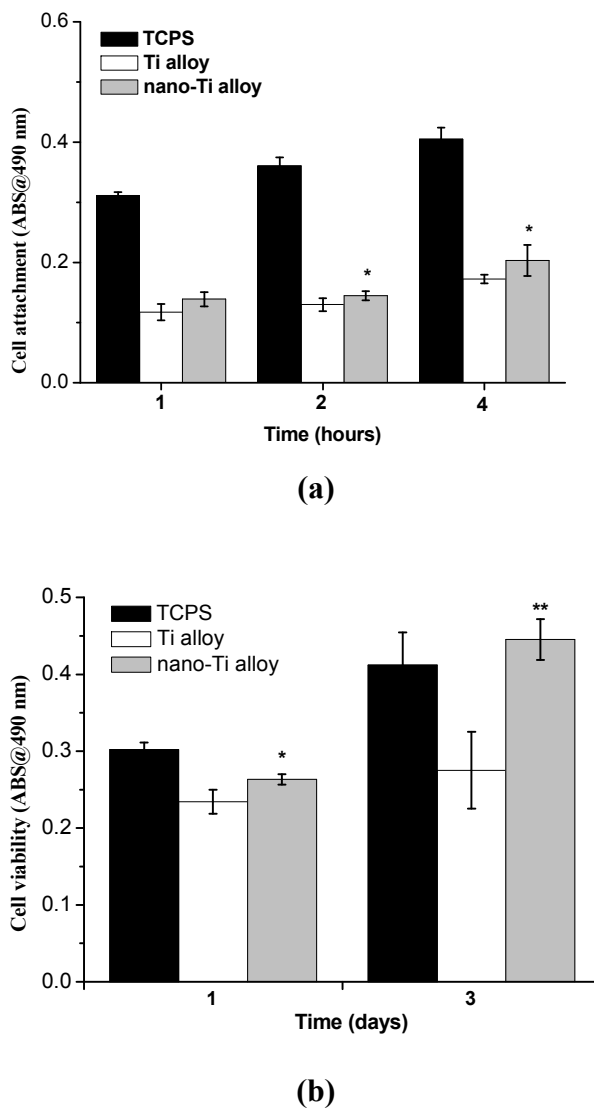


Figure 6. MTT assay. Formazan absorbance indirectly reflects (a) cell initial attachment and (b) cell viability from HUVEC cultured onto native Ti alloy (Ti alloy); surface nanostructured titanium alloy (nano-Ti alloy); and tissue culture polystyrene (TCPS) substrates. Error bars represent means \pm SD for $n = 5$, * $p < 0.05$, ** $p < 0.01$.

3.4. Cell functions

To further investigate the function of HUVECs grown on the native, surface nanostructured titanium alloy substrates, and tissue culture polystyrene (TCPS), we measured NO and prostacyclin (PGI₂) produced by HUVECs. Nitric oxide (NO), an endothelial derived relaxing factor (EDRF),

plays a critical role in regulating vascular tone, relaxing of vascular tissue strips and preventing platelet aggregation [28-30]. It could promote EC growth [31,32], migration [32,33] and angiogenesis [33]. The NO production of HUVECs grown on different substrates was shown in Fig 7. There was no difference between cells cultured on native and surface nanostructured titanium alloy substrates after culture for 1 day. However, the HUVECs cultured on the surface nanostructured titanium alloy displayed significantly higher ($p < 0.01$) NO production than those on the native titanium alloy after culture for 3 days. The result suggests that surface nanostructured titanium alloy promoted the NO production of HUVECs.

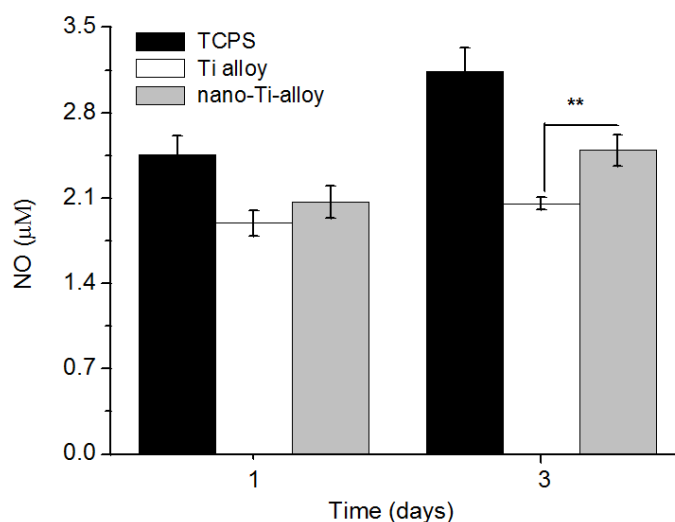


Figure 7. NO production of HUVEC cultured on different substrates. Error bars represent means \pm SD for $n=5$, * $p < 0.05$, ** $p < 0.01$.

Prostacyclin (PGI_2), an unstable prostaglandin, plays an important role in inhibiting platelet aggregation, serotonin release, and leading to vasodilation [30]. Figure 8 shows the PGI_2 production of HUVECs grown on different substrates. There was no statistical difference between cells on the native and surface nanostructured titanium alloy after culture for 1 day. However, the HUVECs cultured on the surface nanostructured titanium alloy displayed statistically higher ($p < 0.05$) PGI_2 production than those on the native titanium alloy after culture for 3 days. This trend was similar to the result of NO production. The above results indicate that the surface nanostructure promoted surface endothelialization.

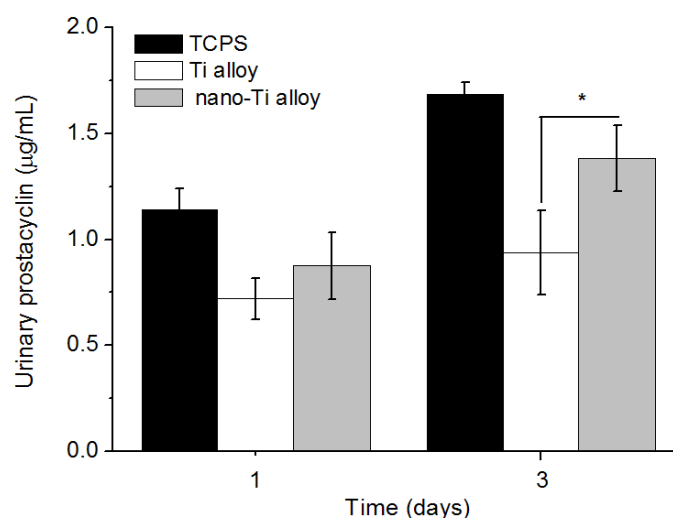


Figure 8. PGI₂ production of HUVEC cultured on different substrates. Error bars represent means \pm SD for n= 5. *p <0.05, **p <0.01.

When a cell ‘feels’ the structural property of the surrounding biomaterial, it would respond correspondingly [26, 34]. The potential mechanism of the present study was proposed as follows: Firstly, after SMAT treatment, the increased fraction of grain boundaries affected the conformation of the adsorbed macromolecules [27], such as fibrinogen from human plasma; Secondly, the adsorbed macromolecules mediated the attachment of the HUVECs, which was speculated from the results of a high level of vinculin expression and enhanced cell initial attachment; Thirdly, the attachment of the HUVECs promoted cell proliferation, in turn affected cell function. Taken together, all results confirm that the surface nanostructured titanium alloy was beneficial for the growth of HUVECs.

4. Conclusion

In this study, we employed surface mechanical attrition treatment technique to exploit surface nanostructured TLM substrates. The successful fabrication of surface nanostructuring of TLM was confirmed by SEM, AFM, TEM, and X-ray diffraction characterizations, respectively. Surface nanostructured TLM substrates improved the growth behaviors of HUVECs, including cell adhesion, proliferation, as well as production of NO and PGI₂. This study affords a platform for understanding the interaction between HUVECs and surface nanostructures of a substrate. Furthermore, it provides an alternative for the fabrication of vascular grafts with high quality.

Acknowledgments

We thank for financial support from Natural Science Foundation of Chongqing Municipal Government (CSTC, 2011JJQ10004 and JJA10056) and Natural Science Foundation of China (51173216 and 31200712).

Conflict of Interest

The authors declare that there are no conflicts of interest related to this study.

References

1. Rabin I, Shani M, Mursi J, et al. (2013) Effect of timing of thrombectomy on survival of thrombosed arteriovenous hemodialysis grafts. *Vasc Endovascular Surg* 47: 342-345.
2. Sista S, Wen C, Hodgson PD, et al. (2011) The influence of surface energy of titanium-zirconium alloy on osteoblast cell functions in vitro. *J Biomed Mater Res Part A*. 97A: 27-36.
3. Blit PH, McClung WG, Brash JL, et al. (2011) Platelet inhibition and endothelial cell adhesion on elastin-like polypeptide surface modified materials. *Biomaterials* 32: 5790-5800.
4. Ranella A, Barberoglou M, Bakogianni S, et al. (2010) Tuning cell adhesion by controlling the roughness and wettability of 3D micro/nano silicon structures. *Acta Biomater* 6: 2711-2720.
5. Seo CH, Furukawa K, Montagne K, et al. (2011) The effect of substrate microtopography on focal adhesion maturation and actin organization via the RhoA/ROCK pathway. *Biomaterials* 32: 9568-9575.
6. Bettinger CJ, Langer R, Borenstein JT. (2009) Engineering substrate topography at the micro- and nanoscale to control cell function. *Angew Chem Int Ed* 48: 5406-5415.
7. Miller DC, Thapa A, Haberstroh KM, et al. (2004) Endothelial and vascular smooth muscle cell function on poly (lactic-co-glycolic acid) with nano-structured surfaces. *Biomaterials* 25: 53-61.
8. Miller DC, Haberstroh KM, Webster TJ. (2007) PLGA nanometer surface features manipulate fibronectin interactions for improved vascular cell adhesion. *J Biomed Mater Res Part A* 81A: 678-684.
9. Choudhary S, Haberstroh KM, Webster TJ. (2007) Enhanced functions of vascular cells on nanostructured Ti for improved stent applications. *Tissue Eng Part A* 13: 1421-1430.
10. Liliensiek SJ, Wood JA, Yong J, et al. (2010) Modulation of human vascular endothelial cell behaviors by nanotopographic cues. *Biomaterials* 31: 5418-5426.
11. Geetha M, Singh AK, Muraleedharan K, et al. (2001) Effect of thermomechanical processing on microstructure of a Ti- 13Nb-13Zr alloy. *J Alloys Compd* 329: 264-271.
12. Kent D, Wang G, Yu Z, et al. (2010) Pseudoelastic behaviour of a [beta] Ti-25Nb-3Zr-3Mo-2Sn alloy. *Mater Sci Eng: A* 527: 2246-2252.
13. Yu ZT, Zhou L. (2006) Influence of martensitic transformation on mechanical compatibility of biomedical β type titanium alloy TLM. *Mater Sci Eng: A* 438-440: 391-394.
14. Tong WP, Tao NR, Wang ZB, et al. (2003) Nitriding iron at lower temperatures. *Science* 299: 686-688.
15. Zhu KY, Vasse A, Brisset F, et al. (2004) Nanostructure formation mechanism of α -titanium using SMAT. *Acta Mater* 52: 4101-4110.
16. Tao NR, Tong WP, Wang ZB, et al. (2003) Mechanical and wear properties of nanostructured surface layer in iron induced by surface mechanical attrition Treatment. *J Mater Sci Tech* 19: 563-566.
17. Wen M, Wen C, Hodgson P, et al. (2011) Wear behavior of pure Ti with a nanocrystalline surface layer. *Appl Mech Mater* 66-68: 1500-1504.

18. Wang ZB, Tao NR, Li S, et al. (2003) Effect of surface nanocrystallization on friction and wear properties in low carbon steel. *Mater Sci Eng A* 352: 144-149.
19. Zhao C, Han P, Ji W, et al. (2012) Enhanced mechanical properties and in vitro cell response of surface mechanical attrition treated pure titanium. *J Biomater Appl* 27:113-118.
20. Zhao CL, Cao P, Ji WP, et al. (2011) Hierarchical titanium surface textures affect osteoblastic functions. *J Biomed Mater Res Part A* 99: 666-675.
21. Lai M, Cai KY, Hu Y, et al. (2012) Regulation of the behaviors of mesenchymal stem cells by surface nanostructured titanium. *Colloids Surf B Biointerfaces* 97: 211-220.
22. Kent D, Wang G, Yu ZT, et al. (2011) Strength enhancement of a biomedical titanium alloy through a modified accumulative roll bonding technique. *J Mech Behav Biomed Mater* 4: 405-416.
23. Paladugua M, Kent D, Wang G, et al. (2010) Strengthening of cast Ti–25Nb–3Mo–3Zr–2Sn alloy through precipitation of α in two discrete crystallographic orientations. *Mater Sci Eng: A* 527: 6601-6606.
24. Zhao C, Han P, Ji W, et al. (2012) Enhanced mechanical properties and in vitro cell response of surface mechanical attrition treated pure titanium. *J Biomater Appl* 27: 113-118.
25. Geiger B, Tokuyasu KT, Dutton AH, et al. (1980) Vinculin, an intracellular protein localized at specialized sites where microfilament bundles terminate at cell membranes. *Proc Natl Acad Sci USA* 77: 4127-4131.
26. Dolatshahi-Pirouz A, Jensen T, Kraft DC, et al. (2010) Fibronectin adsorption, cell adhesion, and proliferation on nanostructured tantalum surfaces. *ACS Nano* 4: 2874-2882.
27. Webster TJ, Schadler LS, Siegel RW, et al. (2001) Mechanisms of enhanced osteoblast adhesion on nanophase alumina involves vitronectin. *Tissue Eng* 7: 291-301.
28. Ignarro LJ, Buga GM, Wood KS, et al. (1987) Endothelium-derived relaxing factor produced and released from artery and vein is nitric oxide. *Proc Natl Acad Sci USA* 84: 9265-9269.
29. Palmer RMJ, Ferrige AG, Moncada S. (1987) Nitric oxide release accounts for the biological activity of endothelium-derived relaxing factor. *Nature* 327: 524-526.
30. Mineo C, Deguchi H, Griffin JH, et al. (2006) Endothelial and antithrombotic actions of HDL. *Circ Res* 98: 1352-1364.
31. Tang JR, Seedorf G, Balasubramaniam V, et al. (2007) Early inhaled nitric oxide treatment decreases apoptosis of endothelial cells in neonatal rat lungs after vascular endothelial growth factor inhibition. *Am J Physiol Lung Cell Mol Physiol* 293: 1271-1280.
32. Cooney R, Hynes SO, Sharif F, et al. (2007) Gene-eluting stents: adenovirus-mediated delivery of eNOS to the blood. *Gene Ther* 14:396-404.
33. Zheng ZZ, Liu ZX. (2007) Activation of the phosphatidylinositol 3-kinase/protein kinase Akt pathway mediates CD151-induced endothelial cell proliferation and cell migration. *Int J Biochem Cell Biol* 39: 340-348.
34. Lu J, Rao MP, MacDonald NC, et al. (2008) Improved endothelial cell adhesion and proliferation on patterned titanium surfaces with rationally designed, micrometer to nanometer features. *Acta Biomater* 4: 192-201.

© 2014, Kaiyong Cai, et al., licensee AIMS Press. This is an open access article distributed under the terms of the Creative Commons Attribution License (<http://creativecommons.org/licenses/by/4.0>)